Experimental study on performance characteristics of Ni-rich NiTi shape memory alloy in wire electric discharge machining (WEDM)

Himanshu Bisaria, Pragya Shandilya*

Mechanical Engineering Department, Motilal Nehru National Institute of Technology Allahabad, Allahabad 211004, India

*Corresponding author

DOI: 10.5185/amp.2018/865
www.vbripress.com/amp

Abstract

Ni-rich NiTi shape memory alloys (SMAs) are gaining more prominence compared to near equiatomic NiTi SMAs due to their excellent superelasticity and shape memory properties. The low density and high work output compared to steels make them an excellent choice for automotive and aerospace industries. The study explores the effect of machining parameters, namely, pulse off time, pulse on time, spark gap voltage, wire tension and wire feed rate on material removal rate (MRR), surface roughness (Ra), and surface morphology of Ni-rich NiTi SMA. The experimental results reveal that MRR & Ra increase with the increase in pulse on time while decrease with the increase in pulse off time and spark gap voltage. Wire feed rate and wire tension have negligible influence on MRR and SR. Surface defects, namely, recast layer, micro-cracks & voids were examined through scanning electron microscope (SEM). Energy dispersive X-ray (EDS) and X-ray diffraction (XRD) analysis results reveal the material transfer from wire electrode and the dielectric fluid on the machined surface.

Keywords: WEDM, $Ni_{55.95}Ti_{44.05}$, SMA, SEM, EDS, XRD.

Introduction

SMAs have been the matter of intensive research since its birth. Ni-rich NiTi SMAs have been widely used in biomedical [1, 2], aerospace and robotics industries [3] due to their unique properties such as shape memory effect, superelasticity, high strength, good corrosion resistance and smooth andsurface properties as compared to equiatomic and near equiatomic NiTi SMAs [4-6]. Machining of SMAs is an important aspect of manufacturing of the several components. However, the machining of SMAs is extremely difficult with conventional machining processes and hence effective and economic processes are required to machine SMAs. Wire electric discharge machining (WEDM) is an advanced machining process based on electrical spark-erosion in which material is removed by means of a series of recurring electrical spark [7, 8]. Over the past few years, WEDM has been widely used for producing the intricate profile with the high surface finish on conductive materials that are difficult to machine by conventional machining [9]. In recent days, WEDM process has been accepted as an effective process for precision machining as well as machining of extremely hard and complex workpiece due to its capability to produce high surface quality, burr-free surfaces, high dimensional accuracy and excellent repeatability [10, 11].

Lin et al. [12], Weinert et al. [13] and Guo et al. [14] were faced similar severe problems such as tool wear, hardening of machined surface, large cutting time and poor surface quality during conventional machining of SMAs. Hsieh et al. [15] explored the machinability of Ti-Ni-Cr/Zr ternary SMA in WEDM and concluded that discharge energy significantly influenced the maximum wire feeding rate. It was also noticed that the machined surface contained Cr_2O_3, TiO_2, $TiNiO_3$, Cu_2O, ZrO_2, Cu–Zn brass and Ni-rich phase. Manjaiah et al. [16] investigated the machinability of equiatomic NiTi SMA during WEDM and observed that the pulse duration was most significant factor followed by flushing pressure and pulse off time. Manjaiah et al. [17] studied the machining characteristics and surface morphology of $Ti_{50}Ni_{45}Cu_5$ SMA in WEDM process. It was noticed that the MRR and surface roughness increased with the increase in peak current, pulse on time and table feed. Liu et al. [18] conducted WEDM on $Ni_{50.8}Ti_{49.2}$ SMA to evaluate the surface integrity from main cut mode to finish trim cut mode. The thick white layer with microcracks in main cut mode and thin white layer without defects in trim cut mode was observed. Liu et al. [19] studied crystallography, composition, and properties of recast layer on $Ni_{50.8}Ti_{49.2}$ SMA machined surface layer in WEDM process. A porous and non-uniform bi-layered structured white layer or recast layer was observed on the

machined surface. The nanohardness of recast layer was found much higher than that of bulk material due to oxide hardening.

From literature survey, it can be found that Very few works have been reported on WEDM of Ni-rich NiTi SMAs. In the present study, the aim of this experimental works is to explore the machinability of $Ni_{55.95}Ti_{44.05}$ SMA in WEDM. The effect of input parameters, i.e., wire tension (WT), wire feed rate (WF), pulse on time (T_{ON}), pulse off time (T_{OFF}) and spark gap voltage (SV) on material removal rate (MRR), surface roughness (SR) and surface morphology was investigated. The energy dispersive X-ray spectroscopy (EDS), X-ray diffraction (XRD) and scanning electron microscope (SEM) techniques were utilized to study the machined surface characteristics of selected samples.

Material and experimental procedure

Materials

Nitinol $Ni_{55.95}Ti_{44.05}$ (55.95 wt. % Ni-44.05 wt. % Ti) square plate with the dimension of 165 mm × 165 mm × 6 mm and density of 6.7 g/cm^3 was selected as a workpiece for this study. The elemental composition of $Ni_{55.95}Ti_{44.05}$ SMA using EDS analysis is shown in **Fig. 1**.

Experimental details

The machining of $Ni_{55.95}Ti_{44.05}$ SMA was performed using four-axis CNC WEDM (Electronica Ultracut, 843). The WEDM parameters such as spark gap voltage, pulse off time, pulse on time, wire feed rate and wire tension were considered input parameters during experimentation. The parameters fixed during machining are shown in **Table 1**. The range of input parameters considered for the experiments is shown in **Table 2**. The specimens with the dimension of 10 mm × 10 mm × 6 mm were machined.

The machining time was calculated by the stopwatch. The MRR was calculated according to equation (1) [20].

$$MRR = Vs \times t \times b \ (mm^3/min) \quad (1)$$

where Vs is cutting speed (mm/min); t is height of sample (mm); b is width of cut (mm) i.e. b = 2Wg+d; Wg is spark gap (mm) and d is wire diameter (mm).

Table 1. Fixed machining parameters in WEDM.

S.No.	Machining parameters	Fixed value
1.	Wire	Brass (Ø 0.25 mm)
2.	Pulse peak voltage	12 V
3.	Servo feed	2060 (mu)
4.	Peak current	2 A
5.	Dielectric (DI-water) pressure	1kg/cm^2
6.	Conductivity of dielectric	±20-24

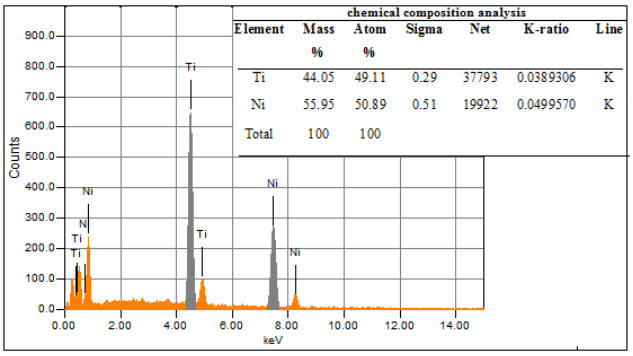

Fig. 1. EDS analysis of $Ni_{55.95}Ti_{44.05}$ SMA.

Table 2. Input variable parameters and their levels.

S.No.	Parameters	Levels				
1.	T_{ON} (µs)	105	110	115	120	125
2.	T_{OFF} (µs)	52	55	57	60	63
3.	SV (V)	35	45	55	65	75
4.	WT (N)	2	4	5	6	8
5.	WF(m/min)	4	6	8	10	12

'Mitutoyo SJ-410' surface roughness tester was used to measure the surface roughness (SR) of the machined surface. The average surface roughness (Ra) of each sample was measured at five different locations and the average was taken as a response parameter. The stylus speed and cutoff length 0.1 mm/s and 0.8 mm respectively were used to evaluate the length of 4 mm. The X-ray analysis of machined surface was conducted on Pan Analytical X'PERT XRD at room temperature using Cu-Kα radiation. The power was 45 kV × 40 mA and the 2θ (5-100°) scanning rate was 2° min^{-1}. The morphological analysis of machined surface was done using JEOL JSM-6010LA SEM equipped with EDS facility. The thickness of the white layer was calculated by using ImageJ software.

Results and discussion

Machining characteristics

The effect of individual process parameters of WEDM on MRR and SR for $Ni_{55.95}Ti_{44.05}$ SMA can be seen from **Fig. 2 (a)** to (e). **Fig. 2 (a)** depicts the variation in pulse on time on MRR and SR. As seen in the **Fig. 2 (a),** at the fixed values of other variable parameters, MRR and SR increase with the increased in pulse on time. At higher pulse on time, the discharge energy and spark's intensity increased which led to more material removal and hence MRR increased [16]. Similarly, at higher electro-discharge energy, deeper craters formed on machined surfaces causing higher SR. **Fig. 2 (b)** represents the effect of with pulse off time on MRR and SR. Both MRR and SR decrease with the increased in the pulse off time. At higher pulse off time, the cooling rate and spark energy decreased, and the time duration between discharge pulses increased causing lower SR and MRR [20]. The effect of spark gap voltage on MRR and SR is shown in **Fig. 2 (c).** The effect of spark gap voltage on MRR and SR is similar to pulse off time. At higher spark

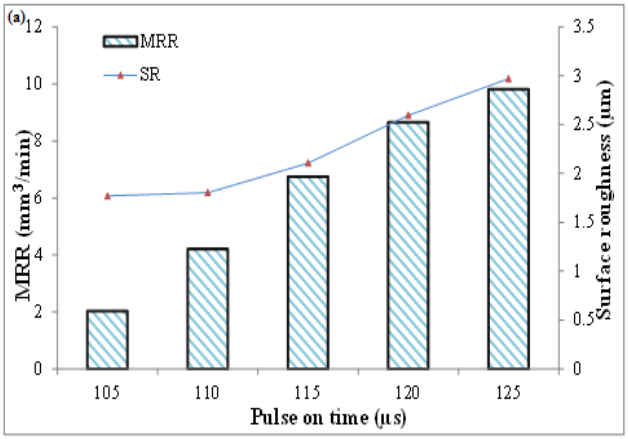

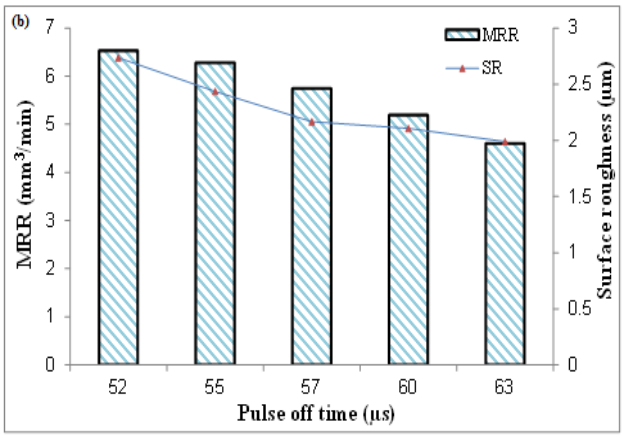

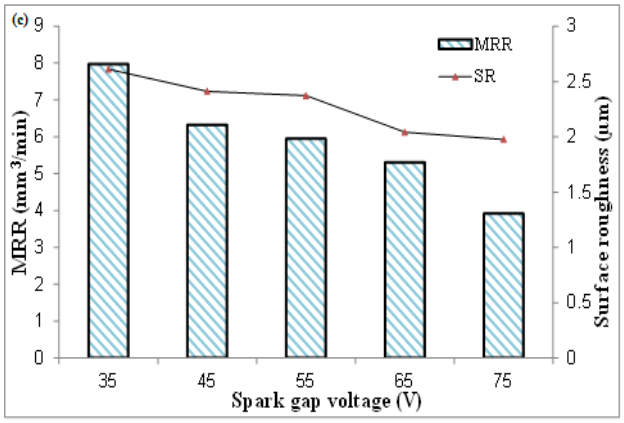

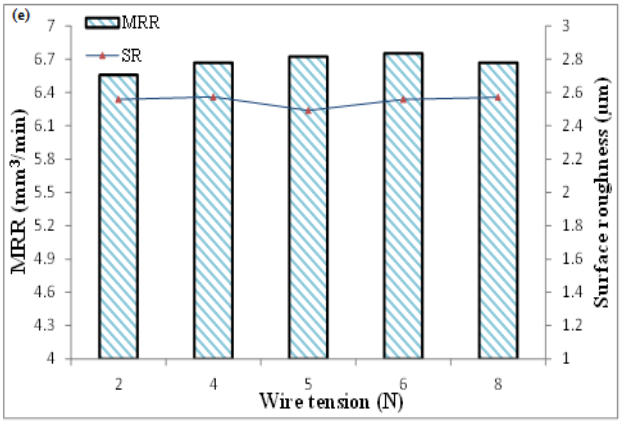

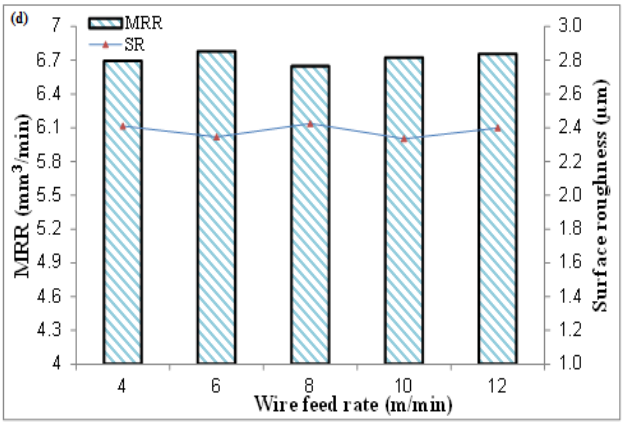

Fig 2. The variation of MRR and surface roughness with (a) pulse on time (b) pulse off time (c) spark gap voltage (d) wire feed rate (e) wire tension.

gap voltage, the spark gap and discharge gap increased and the number of spark per unit time decreased hence leading to lower MRR and SR. **Figs. 2 (d)** and **(e)** show the variation of MRR and SR against wire feed rate and wire tension respectively. Both wire feed rate and wire tension have the negligible effect on MRR and SR. MRR and SR slightly varied with wire feed rate and wire tension. The cost of machining is associated with wire feed rate, for economic machining lower feed rate preferred. A sufficient wire tension is required for accurate machining of $Ni_{55.95}Ti_{44.05}$ SMA in WEDM process.

Surface characteristics

Fig. 3 depicts the SEM micrographs of $Ni_{55.95}Ti_{44.05}$ SMA after WEDM process at higher pulse on time (125). The machined surface is characterized by a melting zone, which is the result of the summation of single spark. Similar to machining characteristics, surface morphology of machined surface depends decisively on the machining parameters of WEDM. As can be seen in **Fig. 3,** many visible discharge craters, globules of debris (melting drops), micro cracks and recast materials are observed on the machined surface after WEDM process. Similar findings were also observed elsewhere [17, 19].

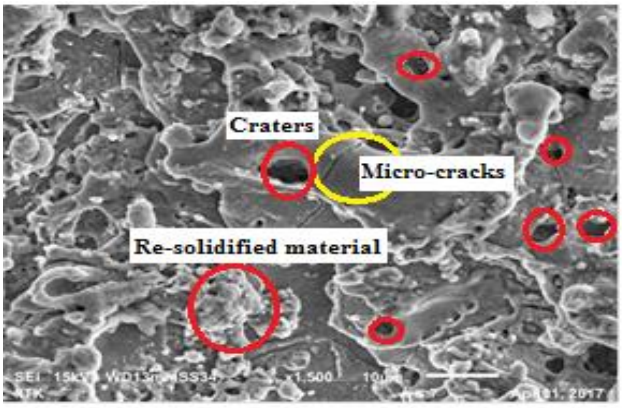

Fig. 3. SEM micrograph of machined surface at higher pulse on time (T_{ON}-125 µs, T_{OFF}-54 µs, SV-50 V, WF-8 m/min and WT-5 N).

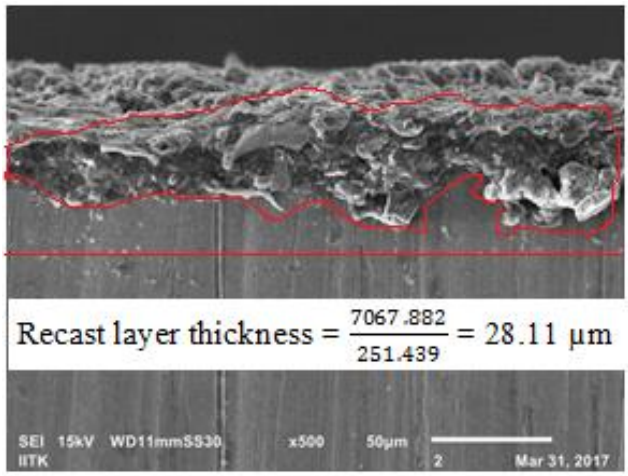

Fig. 4. Recast layer formed on machined surface at higher pulse on time (T_{ON}-125 µs, T_{OFF}-54 µs, SV-50 V, WF-8 m/min and WT-5 N).

Recast layer analysis

Fig. 4 represents the white layer thickness or recast layer thickness of cross-sectioned specimen after WEDM process. The qualitative analysis of recast layer has been accomplished by EDS analysis as shown in **Fig. 4**. The EDS analysis result reveals that the recast layer comprises the atoms of C, Cu, Zn, O, Ni and Ti. The presence of another element besides Ni and Ti in recast layer is due to chemical reaction at the higher temperature. In WEDM process, elements from both brass wire (Cu and Zn) and dielectric might be diffused into the machined surface.

XRD phase analysis

Fig. 5 illustrates the XRD pattern of the machined surface layer for $Ni_{55.95}Ti_{44.05}$ SMA after WEDM process. The machined surface layer consists of Nitinol, Ni (TiO_3), TiO_2, $Ti2O_3$, Ni_3Ti, Cu-Zn brass and Ni-rich phase. The high reactivity of Ti and Ni atoms is ascribed to the formation of oxides of Ni and Ti oin the layer of the machined surface. The formation of the compound of Cu and Zn is due to the diffusion of Cu and Zn from the brass wire into the machined surface. The diffusion of residual Ni atoms into NiTi matrix led to the formation of Ni-rich phase.

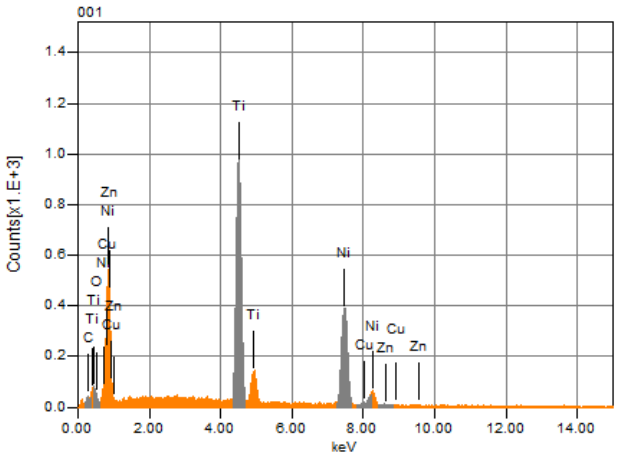

Fig. 5. EDS analysis of recast layer.

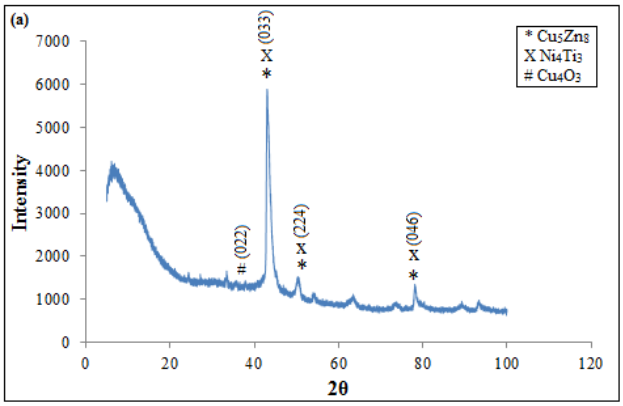

Fig. 5. XRD pattern of machined surface of $Ni_{55.95}Ti_{44.05}$ SMA at higher pulse on time (T_{ON}-125 µs, T_{OFF}-54 µs, SV-50 V, WF-8 m/min and WT-5 N).

Conclusion

The following conclusions can be drawn based on experimental results and analysis:

(1) MRR and surface roughness increase by increasing pulse on time and decrease by increasing pulse off time and spark gap voltage. Whereas, wire feed rate and wire tension have the trifling effect.

(2) The machined surface is characterized by imperfections such as many debris, micro-cracks, voids and re-solidified molten material.

(3) The EDS analysis of recast layers divulges the migration of foreign elements atoms (Cu, Zn, C and O) from brass wire and dielectric fluid on the recast layer near the machined surface.

(4) XRD analysis of machined surface reveals that the various oxides and chemical compounds of Cu, Zn, Ni and Ti namely Cu_5Zn_8, Ni_4Ti_3, and Cu_4O_3 identified on machined surface after WEDM.

Acknowledgements

The author would like to thank ACMS department IIT Kanpur, Kanpur for providing SEM and XRD facility for accomplishing this work.

References

1. Jani, J.M.; Leary, M.; Subic, A.; Gibson, M. A.; *Mater Design*, **2014**, 56, 1078. **DOI:** 10.1016/j.matdes.2013.11.084
2. Marchand, C.; Heim, F.; Durand, B.; Chafke, N.; *Mater. Manuf. Processes*, **2011**, 26, 181. **DOI:** 10.1080/10426914.2010.491695
3. Manjaiah, M.; Narendranath, S.; Basavarajappa, S.; *T Nonferr Metal Soc.*, **2014**, 24, 12. **DOI:** 10.1016/S1003-6326(14)63022
4. Petrini, L.; Migliavacca, F.; *Journal of Metallurgy* **2011**, 15. **DOI:** 10.1155/2011/501483.
5. Ramachandran, B.; Chen, C.H.; Chang, P.C.; Kuo, Y.K.; Chien, C.; Wu, S. K.; *Intermetallics* **2015**, 60, 79. **DOI:** 10.1016/j.intermet.2015.02.004
6. Karimzadeh M, Aboutalebi MR, Salehi MT Abbasi S.M.; Morakabati M.; *Mater. Manuf. Processes*, **2016**, 31, 1014. **DOI:** 10.1080/10426914.2015.1048468
7. Mandal, A.; Dixit, A.R.; Das, A.K.; Mandal, N.; *Mater. Manuf. Processes*, **2016**, 31, 860-866.
8. Pramanik, A.; Islam, M.N.; Boswell, B.; Basak, A.K.; Dong, Y.; Littlefair, G.; *Proc IMechE, Part B: J Engineering Manufacture*, **2016**. **DOI:** 10.1177/0954405416662079

9. Giridharan, A.; Samuel, G.L.; *Proc IMechE, Part B: J Engineering Manufacture*, **2015,** 230, 2064.
DOI: 10.1177/0954405415615732
10. Rao, M.S.; Venkaiah, N.; *Proc IMechE, Part B: J Engineering Manufacture*, **2016.**
DOI: 10.1177/0954405416654092
11. Gupta, K.; Jain, N. K.; *J. Mater. Manuf. Processes*, **2013**, 28, 1153.
DOI: 10.1080/10426914.2013.792422
12. Lin, H.C.; Lin, K.M.; Chen, Y.C.; *J. Mater. Process. Technol*,. **2000,** 105, 327.
DOI: 10.1016/S0924-0136(00)00656-7
13. Weinert, K.; Petzoldt, V.; Kotter, D.; *CIRP Annals-Manufacturing Technology*, **2004**, 53, 65.
DOI: 10.1016/S0007-8506(07)60646-5
14. Guo Y.; Klink, A.; Fu, C.; Snyder, J. *CIRP Annals Manufacturing Technology*, **2013,** 62, 83.
DOI: 10.1016/j.cirp.2013.03.004
15. Hsieh, S. F.; Chen, S. L.; Lin, H. C.; Lin, M. H.; Chiou, S. Y.; INT J MACH TOOL MANU.; **2009,** 49, 509.
DOI: 10.1016/j.ijmachtools.2008.12.013
16. Manjaiah, M.; Narendranath, S.; Basavarajappa, S.; Gaitonde, V. N.; *Trans. Nonferrous Met. Soc. China*, **2014,** 24, 3201.
DOI: 10.1016/S1003-6326(14)63461-0
17. Manjaiah M.; Narendranath, S.; Basavarajappa, S.; *Silicon* **2016**, 8, 467.
DOI: 10.1007/s12633-014-9273-4
18. Liu, J.F.;, Li, L.; Guo, Y.B..; *Procedia CIRP*, **2014,** 13, 137.
DOI: 10.1016/j.apsusc.2014.04.146
19. Liu, J. F.; Guo, Y.B., Butler, T.M.; Weaver, M. L.; *Mater Design*, **2016,** 109, 1.
DOI: 10.1016/j.matdes.2016.07.063
20. Manjaiah, M., Narendranath, S.; Basavarajappa, S.; Gaitonde V.N.; Precis. Eng. 2015; 41, 68.
DOI: 10.1016/j.precisioneng.2015.01.008

.

